MOLECULAR AND CELLULAR BIOLOGY, Nov. 2003, p. 8202–8215 Vol. 23, No. 22
0270-7306/03/$08.00+0 DOI: 10.1128/MCB.23.22.8202–8215.2003

The Ku Heterodimer Performs Separable Activities at Double-Strand Breaks and Chromosome Termini

Alison A. Bertuch[1,2]* and Victoria Lundblad[2]

Department of Pediatrics, Hematology/Oncology Section,[1] and Department of Molecular and Human Genetics,[2] Baylor College of Medicine, Houston, Texas 77030

Received 14 March 2003/Returned for modification 28 April 2003/Accepted 7 August 2003

The Ku heterodimer functions at two kinds of DNA ends: telomeres and double-strand breaks. The role that Ku plays at these two classes of termini must be distinct, because Ku is required for accurate and efficient joining of double-strand breaks while similar DNA repair events are normally prohibited at chromosome ends. Toward defining these functional differences, we have identified eight mutations in the large subunit of the Saccharomyces cerevisiae Ku heterodimer (*YKU80*) which retain the ability to repair double-strand breaks but are severely impaired for chromosome end protection. Detailed characterization of these mutations, referred to as *yku80^{tel}* alleles, has revealed that Ku performs functionally distinct activities at subtelomeric chromatin versus the end of the chromosome, and these activities are separable from Ku's role in telomere length regulation. While at the chromosome terminus, we propose that Ku participates in two different activities: it facilitates telomerase-mediated G-strand synthesis, thereby contributing to telomere length regulation, and it separately protects against resection of the C-strand, thereby contributing to protection of chromosome termini. Furthermore, we propose that the Ku heterodimer performs discrete sets of functions at chromosome termini and at duplex subtelomeric chromatin, via separate interactions with these two locations. Based on homology modeling with the human Ku structure, five of the *yku80^{tel}* alleles mutate residues that are conserved between the yeast and human Ku80 proteins, suggesting that these mutations probe activities that are shared between yeast and humans.

Telomeres are essential structures that constitute the ends of linear chromosomes. In the majority of eukaryotes studied, telomeric DNA consists of tandem arrays of simple G-rich sequence which are maintained by the enzyme telomerase (39). The G-rich strand extends 5′ to 3′ toward the chromosome end, terminating in a single-stranded 3′ overhang. The assembly of both duplex and single-strand telomeric DNA binding proteins onto telomeric DNA gives rise to a nonnucleosomal structure. A primary function of this telomeric nucleoprotein complex is to prevent the natural chromosome ends from being subject to DNA repair and recombination activities, thereby preventing end-to-end fusions and unregulated resection of terminal DNA sequences (10). In contrast, DNA ends created by double-strand breaks (DSBs) are targets for repair activities, thus averting the toxic consequences to the genome if a DSB is left unrepaired (19).

In the nonhomologous end-joining (NHEJ) pathway of DSB repair, broken ends with little or no sequence homology are joined with minimal, if any, sequence loss (32). In both *Saccharomyces cerevisiae* and higher eukaryotes, the Ku heterodimer is required for this process to occur both accurately and efficiently (6, 40). Consisting of 70- and 80-kDa subunits, this abundant heterodimeric complex binds with high affinity to DNA ends in a sequence-independent fashion and to a variety of terminal structures, such as blunt ends and 3′ overhangs (15). As predicted by its known in vitro binding properties, Ku localizes to DSBs in vivo (38). Biochemical studies suggest that Ku acts at DSBs as a bridging complex, an alignment factor, and a recruitment factor in the end-fusing process (18, 27, 42, 46, 51). Additionally, in yeast cells, there is enhanced degradation of broken chromosomes in the absence of Ku, suggesting a role for Ku in the protection of DNA ends from nucleolytic processing (29).

Unexpectedly, the Ku heterodimer also localizes to telomeres in both yeast and mammalian cells, and loss of Ku function results in dysfunctional telomeres across species (20, 23). Disruption of Ku activity in budding yeast cells, due to mutations in either of the Ku subunits (encoded by *YKU70* and *YKU80*), results in a number of telomere-related phenotypes, suggesting that Ku has multiple activities at chromosome ends. First, Ku is required for telomere length regulation (50), an activity that is mediated through a 48-nucleotide stem-loop structure of TLC1, the RNA subunit of yeast telomerase (48, 55). In addition, Ku contributes to yeast telomeric chromatin structure, as expression of a telomeric reporter gene is altered in strains that lack either *YKU70* or *YKU80* (5, 28, 43).

The Ku heterodimer also makes critical contributions to the protection of chromosome ends. In budding yeast cells, Ku protects telomeres from homologous recombination (14). In addition, regulation of the terminal G-rich single-strand overhang is lost in Ku-deficient strains (20, 49) due to unregulated resection of the telomeric C-rich strand (37). Furthermore, budding yeast strains deficient in both telomerase (e.g., due to loss of *EST2*, the telomerase catalytic subunit, or *EST1*, a telomerase regulatory subunit) and Ku display a greatly accelerated senescence progression compared to that exhibited by a telomerase-deficient strain (20, 43, 49). Similarly, rapid loss of telomeric DNA and decreased survival have also been observed in fission yeast strains that lack both Ku and telomerase

* Corresponding author. Mailing address: Department of Pediatrics, Baylor College of Medicine, One Baylor Plaza, Houston, TX 77030. Phone (832) 824-4579. Fax: (832) 825-4657. E-mail: abertuch@bcm.tmc.edu.

(4). The inviability displayed by these double-mutant strains is thought to be due to the simultaneous inability to both replicate and protect chromosome ends (A. Bertuch and V. Lundblad, submitted for publication). Ku has also been implicated in chromosome end protection in mouse cells, based on the increase in chromosomal end-to-end fusions that are observed in the absence of Ku function (3, 9, 23, 53). Moreover, the degree of telomeric dysfunction observed in Ku-deficient cells, as measured by end-to-end fusions, is comparable to that observed in late-generation telomerase-deficient mice (16).

Insight into Ku's function at a molecular level has come from the determination of the crystal structure of the human Ku heterodimer, both alone and in complex with a DNA substrate (61). These structures reveal that the Ku70 and Ku80 protein subunits share a three-domain topology, with each comprised of an N-terminal α/β domain, a central β-barrel domain and a C-terminal arm. The associated subunits give rise to a quasi-symmetric basket-like molecule with a narrow preformed ring, which cradles and encircles the DNA. The N-terminal α/β domains, which lie at the periphery of the heterodimer, contribute minimally to heterodimerization or DNA binding and are potentially involved in interactions with other proteins. Together, the β-barrel domains form the DNA binding surface and the ring-like structure through which the duplex DNA is threaded. Last, the helical C-terminal arms of each subunit are positioned to contact the β-barrel of the opposite subunit, thereby contributing to heterodimerization. The structure of the heterodimer-DNA complex can be readily incorporated with current models of Ku function in NHEJ. For example, the ring-like structure is consistent with its requirement for DNA ends, and the absence of specific contacts with DNA bases explains its sequence-independent mode of binding. The positioning of the DNA helix fits well with a role for Ku as an alignment factor, yet the ends are left accessible to end processing events. How the Ku heterodimer dissociates from a DNA end once end joining has occurred and whether translocation occurs in vivo, as has been observed in vitro (11), are questions that have not yet been resolved.

The dual requirement at DSBs, where Ku promotes end-to-end fusions, and at telomeres, which are specifically protected from end joining, presents a paradox. What prevents Ku from mediating the same kinds of events at telomeres that it promotes at DSBs? A possible resolution of this paradox is a model in which Ku performs different activities at these two different classes of DNA ends. For example, telomere-specific proteins could modulate an activity performed by Ku when it is associated with chromosome ends that is precluded from occurring at DSBs. To test this model, we asked whether mutations in *YKU80* that separate its DNA repair function from its telomere function could be recovered. We report here the identification of mutations, called *yku80^{tel}* alleles, which result in striking defects in telomere maintenance but are still proficient for DNA repair. This supports a model in which Ku performs different activities at these two different types of ends. Furthermore, the *yku80^{tel}* mutations differentially impact telomere length regulation, telomere end protection, and telomeric silencing, suggesting that Ku has separable functions at the telomere as well. Based on sequence alignment and homology modeling with the human Ku structure, four of the mutated residues map to within the N-terminal α/β domain. Because this domain has been proposed to mediate interactions between Ku and other factors (61), we suggest that this is a region that is critical for telomere-specific interactions.

MATERIALS AND METHODS

Yeast strains and plasmids. The *S. cerevisiae* strains used in this work (Table 1) are isogenic derivatives of YPH275 (from Phil Hieter), UCC3505 (54), or JKM179 (29). The *yku80*-Δ::*kan^r*, *est1*-Δ::*HIS3*, *est2*-Δ::*URA3*, *tlc1*-Δ::*LEU2*, *cdc13-2*, and *tlc1*-Δ*48* mutations have been previously described (31, 34, 43, 44, 48). The *rad52*-Δ::*LYS2* disruption (pVL392) removes amino acids (aa) 141 to 260 of the *RAD52* open reading frame (ORF). The *rif1*-Δ::*TRP1* mutation removes the entire *RIF1* ORF, and the *rif2*-Δ::*HIS3* mutation removes the entire *RIF2* ORF and 55 bp of upstream sequence.

The *yku80*-Δ *rad52*-Δ strain used for Fig. 1A and the *yku80*-Δ strains used for Fig. 2C, D, and E, 3A and B, and 5D, were generated by sporulation of YVL194. Strains YVL885 and YVL2073 were generated by introducing *yku80*-Δ::*kan^r* mutations into UCC3505 (54) and JKM179 (29), respectively. YVL869, used in the first screen, was derived by sporulation of YVL235. YVL918, used in the second screen, was constructed from YVL885 by introducing a *tlc1*-Δ::*LEU2* mutation (in the presence of pVL1037 [*CEN TRP1 YKU80*]), transforming the strain with pVL1312 (*CEN LYS2 TLC1*), and subsequently losing plasmid pVL1037. YVL1041 was derived by transforming YVL464 with pVL232 (*CEN URA3 EST1*) and obtaining the desired genotype by sporulation. YVL1071 was generated by sequentially introducing *rif2*-Δ::*HIS3* and *rif1*-Δ::*TRP1* into YVL463. To generate YVL1079, the *tlc1*-Δ*48* mutation was integrated into a haploid derived from sporulation of YPH275 utilizing plasmid pRS306-*tlc1*-Δ*48* (48). Strains YVL2053, YVL2054, YVL2055, YVL2068, YVL2069, YVL2070, and YVL2108 were generated by integrating the relevant *yku80^{tel}* mutant allele into the genome of a wild-type haploid derived from YPH275 by utilizing plasmids pVL2048, pVL2050, pVL1070, pVL2084, pVL2085, pVL1807, and pVL1870, respectively. The haploid strains were mated to a freshly dissected *est1*-Δ::*HIS3* isogenic haploid to obtain the double heterozygous diploids.

The plasmids used in this work are described in Table 2. Plasmid pVL1037 contains the genomic *YKU80* ORF and flanking sequence subcloned into pRS414 (*CEN TRP1*). XL1-Red mutagenesis (Stratagene) of pVL1037 yielded pVL1078, pVL1765, pVL1766, pVL1079, pVL1693, pVL1694, pVL1695, and pVL1696, which contain the *yku80-1* through *yku80-8* alleles, respectively. The *yku80^{tel}* inserts from these plasmids and the *YKU80* insert from pVL1037 were subcloned into pRS415 (*CEN LEU2*).

To integrate the *yku80^{tel}* mutant alleles, *yku80-1* and *yku80-8*, and derivatives of *yku80-2*, *yku80-3*, *yku80-4*, *yku80-6*, and *yku80-7*, which contained additional restriction sites that did not alter the protein sequence, were subcloned into pRS406 (*URA3*). The *yku80-1* and *yku80-8* mutations introduce unique restriction sites (*Nla*III and *Hpa*I, respectively) and, therefore, were directly subcloned into pRS406 to generate pVL1070 and pVL1807, respectively. Site-directed mutagenesis was performed to introduce or eliminate restriction sites by silent mutation adjacent to the *yku80-2* (*Pvu*II site), *yku80-3* (*Cla*I site), *yku80-6* (*Hph*I site), and *yku80-7* (loss of *Bst*UI site) mutations. These alleles were subcloned into pRS406 to generate pVL2050, pVL2048, pVL2084, and pVL2085, respectively. A similar strategy was employed for *yku80-4* (*Ear*I site) to generate pVL1870. In addition, the C-terminal region of *yku80-4* was truncated to facilitate integration of the *yku80-4* mutation.

Plasmid pVL1069 contains the *YKU80* insert from pVL1037 subcloned into pRS416 (*CEN URA3*). Plasmid pVL1352, a *YKU80$_{myc18}$* derivative of pVL1069, was generated by subcloning an 18-myc epitope tag in frame with the C terminus of *YKU80* with pJBN130. A similar approach was used to construct *yku80-1$_{myc18}$* through *yku80-8$_{myc18}$* plasmids.

Identification of separation-of-function alleles of *YKU80*. The first mutant screen yielded mutations *yku80-1* through *yku80-4*. Plasmid pVL1037 (*CEN TRP1 YKU80*) was mutagenized by passage through XL1-Red cells (Stratagene). An average of 1 mutation was introduced per 2,000 bp. The mutant plasmid library was transformed into YVL869 and plated on −Trp −Ura medium (i.e., medium lacking tryptophan and uracil). A total of 15,700 colonies were plated. Colony growth following loss of the *TLC1* plasmid was monitored by two successive replica platings onto −Trp 5-fluoroorotic acid (5-FOA) media. Strains showing a reduced growth or synthetic lethal phenotype (104 in total) were recovered from the −Trp −Ura plates, and the mutant *yku80* plasmids were rescued. In the second step of the screen, these plasmids were introduced into a *MAT***a** *yku80*-Δ::*kan^r* *rad52*-Δ::*LYS2* strain and tested for NHEJ by the in vivo plasmid repair assay (see below). Four plasmids exhibited robust in vivo plasmid repair activity and were further characterized.

TABLE 1. Strain list

Strain	Genotype
YVL194[a]	*MAT***a** *yku80-*Δ::*kan*^{r} *cdc13-2* *rad52-*Δ::*LYS2* / *MAT*α *YKU80* *CDC13* *RAD52*
YVL235[a]	*MAT***a** *yku80-*Δ::*kan*^{r} *tlc1-*Δ::*LEU* *pSD120* (*CEN URA3 TLC1*) / *MAT*α *YKU80* *TLC1*
YVL463[a]	*MAT***a** *yku80-*Δ::*kan*^{r} *est2-*Δ::*URA3* / *MAT*α *YKU80* *EST2*
YVL464[a]	*MAT***a** *yku80-*Δ::*kan*^{r} *est1-*Δ::*HIS3* CF (*ura3*::*TRP1 SUP11 CEN4 D8B*) / *MAT*α *YKU80* *EST1*
YVL869[a]	*MAT*α *yku80-*Δ::*kan*^{r} *tlc1-*Δ::*LEU2* pSD120 (*CEN URA3 TLC1*)
YVL1041[a]	*MAT***a** *yku80-*Δ::*kan*^{r} *est1-*Δ::*HIS3* pVL232 (*CEN URA3 EST1*)
YVL1071[a]	*MAT***a** *yku80-*Δ::*kan*^{r} *est2-*Δ::*URA3* *rif1-*Δ::*TRP1* *rif2-*Δ::*HIS3* / *MAT*α *YKU80* *EST2* *RIF1* *RIF2*
YVL1079[a]	*MAT***a** *tlc1-*Δ*48* CF (*ura3*::*TRP1 SUP11 CEN4 D8B*)
YVL2053[a]	*MAT***a** *yku80-3* *est1-*Δ::*HIS3* CF (*ura3*::*TRP1 SUP11 CEN4 D8B*) / *MAT*α *YKU80* *EST1*
YVL2054[a]	*MAT***a** *yku80-2* *est1-*Δ::*HIS3* CF (*ura3*::*TRP1 SUP11 CEN4 D8B*) / *MAT*α *YKU80* *EST1*
YVL2055[a]	*MAT***a** *yku80-1* *est1-*Δ::*HIS3* CF (*ura3*::*TRP1 SUP11 CEN4 D8B*) / *MAT*α *YKU80* *EST1*
YVL2068[a]	*MAT***a** *yku80-6* *est1-*Δ::*HIS3* / *MAT*α *YKU80* *EST1*
YVL2069[a]	*MAT***a** *yku80-7* *est1-*Δ::*HIS3* / *MAT*α *YKU80* *EST1*
YVL2070[a]	*MAT***a** *yku80-8* *est1-*Δ::*HIS3* CF (*ura3*::*TRP1 SUP11 CEN4 D8B*) / *MAT*α *YKU80* *EST1*
YVL2108[a]	*MAT***a** *yku80-4* *est1-*Δ::*HIS3* CF (*ura3*::*TRP1 SUP11 CEN4 D8B*) / *MAT*α *YKU80* *EST1*
YVL885[b]	*MAT***a** *yku80-*Δ::*kan*^{r} *ura3-52 lys2-801 ade2-101 trp1-*Δ*63 his3-*Δ*200 leu2-*Δ*1 ppr1*::*HIS3 adh4*::*URA3*-(*URA3* at TEL VII_L) DIA5-1 (*ADE2* at TEL V_R)
YVL918[b]	*MAT***a** *yku80-*Δ::*kan*^{r} *tlc1-*Δ::*LEU2 can1-*Δ::*GAL-Eco*RI *ura3-52 lys2-801 ade2-101 trp1-*Δ*63 his3-*Δ*200 leu2-*Δ*1 ppr1*::*HIS3 adh4*::*URA3*-(*URA3* at TEL VII_L) DIA5-1 (*ADE2* at TEL V_R) pVL1312 (*CEN LYS2 TLC1*)
YVL2073[c]	*MAT*α *yku80-*Δ::*kan*^{r} *hml-*Δ::*ADE1 hmr-*Δ::*ADE1 ade1 lys5 leu2 ura3-52 trp1-*Δ::*hisG′ ADE3*::*GAL*::*HO*

[a] Isogenic derivative of YPH275 (from Phil Hieter). Diploid strains carry *ura3-52*/*ura3-52 lys2-801*/*lys2-801 ade2-101*/*ade2-101 trp1-*Δ*1*/*trp1-*Δ*1 his3-*Δ*200*/*his3-*Δ*200 leu2-*Δ*1*/*leu2-*Δ*1*, and haploid strains carry *ura3-52 lys2-801 ade2-101 trp1-*Δ*1 his3-*Δ*200 leu.* The chromosome fragment (CF) is in the designated strains in single copy.
[b] Isogenic derivative of UCC3505 (54).
[c] Isogenic derivative of JKM179 (29).

The second mutant screen, which yielded mutations *yku80-5* through *yku80-8*, monitored for the loss of telomeric silencing with a telomeric *ADE2* reporter assay and subsequent growth after loss of a *TLC1* covering plasmid. YVL918 was transformed with the mutagenized pVL1037 plasmid library described above and plated on −Trp −Lys media. A total of 16,600 colonies were plated. The loss of telomeric position effect was monitored by replica plating to limiting Ade −Trp −Lys medium. Growth after loss of the *TLC1* covering plasmid was monitored by replica plating to −Trp α-aminoadipate media. Strains that were white on the limiting Ade plates (indicating expression of the normally repressed *ADE2* gene) and grew on the α-aminoadipate plates were recovered from the −Trp −Lys plates, and the mutant plasmids were rescued. A total of 99 transformants underwent quantitative testing. Plasmids were rescued from 15 transformants of interest, and of these, 4 retested and were further characterized.

Genetic methods. All incubations were performed at 30°C unless otherwise noted. For the −Trp α-aminoadipate plates, the final concentration of the α-aminoadipic acid was 0.05% (58). Telomere Southern blots were performed as previously described (31). The mean telomere lengths were calculated by averaging the length of the Y′-containing telomere band (e.g., see the bracket in Fig. 3A), which represents roughly two-thirds of the yeast telomeres, for four independent isolates of each allele and subtracting the length of the Y′ nontelomeric sequence (870 bp).

To analyze the growth phenotype of *yku80^{tel} est1-*Δ double mutants following sporulation and dissection, the appropriate double heterozygous diploids (YVL464, YVL2053, YVL2054, YVL2055, YVL2068, YVL2069, YVL2070, and VL2108) were sporulated at ~23°C. Dissection plate colonies were resuspended, cell counts were performed, and cells were diluted to equivalent concentrations. Tenfold serial dilutions were plated onto rich media and grown at 28°C.

To analyze the growth phenotype of *yku80^{tel} est1-*Δ double mutants following plasmid shuffle, YVL1041 was transformed with pRS414-based plasmids containing *YKU80* or *yku80^{tel}* mutant alleles or empty vector and grown to saturation in media selecting for both the *EST1* (*URA3*) and *yku80* (*TRP1*) plasmids. Saturated cultures were used to inoculate media selecting for the *TRP1* plasmids only and grown overnight. Tenfold serial dilutions were plated on −Trp −Ura (to confirm equivalent plating efficiency) and −Trp 5-FOA. Plates were examined after 2 to 3 days at 30°C.

For the analysis of telomere silencing, YVL885 was transformed with plasmids containing *YKU80* or *yku80^{tel}* mutant allele derivatives of pRS414 or empty vector and grown to mid-log phase in media selecting for the *yku80* (*TRP1*) plasmids. To monitor the telomeric *URA3* reporter, 10-fold serial dilutions were plated on −Trp, −Trp −Ura, and −Trp 5-FOA plates. Growth was assessed after 2 to 3 days at 30°C. To monitor the telomeric *ADE3* reporter, YVL885 was transformed with plasmids containing *YKU80* or *yku80^{tel}* mutant allele derivatives of pRS415 or empty vector and grown to mid-log phase in media selecting for the *yku80* (*LEU2*) plasmids. The strains were plated for single colonies on −Leu plates with limiting adenine and allowed to grow to full size for 3 days at 30°C. The plates were stored at 4°C prior to photography to enhance detection of red pigment.

NHEJ assays. The previously described in vivo plasmid repair assay (7) was modified as follows. A *MAT***a** *yku80-*Δ::*kan*^{r} *rad52-*Δ::*LYS2* strain was transformed with *yku80^{tel}* mutant derivatives of pRS414 and wild-type and vector controls. Individual transformants were cotransformed with equivalent amounts of linearized pRS413 (*CEN HIS3*) and supercoiled pRS415 (*CEN LEU2*). Transformation reactions were divided and plated on −Trp −His and −Trp −Leu media. Colonies were counted and the Ura^+/Leu^+ transformant ratio was determined. The average value for each *yku80* allele was normalized to the average value for the wild type.

The HO endonuclease assay was performed by transforming YVL2073 with *yku80^{tel}* mutant allele derivatives of pRS415 and wild-type and vector controls. Tenfold serial dilution of cells were plated on glucose −Leu and galactose −Leu plates.

TABLE 2. Plasmid list

Plasmid	Description	Source or reference
pVL1037	*CEN TRP1 YKU80*	pRS414
pVL1078	*CEN TRP1 yku80-1*	pVL1037
pVL1765	*CEN TRP1 yku80-2*	pVL1037
pVL1766	*CEN TRP1 yku80-3*	pVL1037
pVL1079	*CEN TRP1 yku80-4*	pVL1037
pVL1693	*CEN TRP1 yku80-5*	pVL1037
pVL1694	*CEN TRP1 yku80-6*	pVL1037
pVL1695	*CEN TRP1 yku80-7*	pVL1037
pVL1696	*CEN TRP1 yku80-8*	pVL1037
pRS414	*CEN TRP1*	8
pVL1067	*CEN LEU2 YKU80*	pRS415
pVL1072	*CEN LEU2 yku80-1*	pVL1067
pVL1855	*CEN LEU2 yku80-2*	pVL1067
pVL1854	*CEN LEU2 yku80-3*	pVL1067
pVL1076	*CEN LEU2 yku80-4*	pVL1067
pVL1859	*CEN LEU2 yku80-5*	pVL1067
pVL1857	*CEN LEU2 yku80-6*	pVL1067
pVL2069	*CEN LEU2 yku80-7*	pVL1067
pVL1860	*CEN LEU2 yku80-8*	pVL1067
pRS415	*CEN LEU2*	8
pVL1070	*URA3 yku80-1*	pRS406
pVL2050	*URA3 yku80-2*$_{(+ClaI\ aa\ 15)}$	pRS406
pVL2048	*URA3 yku80-3*$_{(+PvuII\ aa\ 46)}$	pRS406
pVL1870	*URA3 yku80-4*$_{(+EarI\ aa\ 437,\ \Delta 522–629)}$	pRS406
pVL2084	*URA3 yku80-6*$_{(+HphI\ aa\ 362)}$	pRS406
pVL2085	*URA3 yku80-7*$_{(-BstUI\ aa\ 438)}$	pRS406
pVL1807	*URA3 yku80-8*	pRS406
pVL1069	*CEN URA3 YKU80*	pRS416
pVL1352	*CEN URA3 YKU80*$_{myc18}$	pRS1069
pVL1353	*CEN URA3 yku80-1*$_{myc18}$	pVL1352
pVL1810	*CEN URA3 yku80-2*$_{myc18}$	pVL1352
pVL1809	*CEN URA3 yku80-3*$_{myc18}$	pVL1352
pVL1354	*CEN URA3 yku80-4*$_{myc18}$	pVL1352
pVL1816	*CEN URA3 yku80-5*$_{myc18}$	pVL1352
pVL1818	*CEN URA3 yku80-6*$_{myc18}$	pVL1352
pVL1817	*CEN URA3 yku80-7*$_{myc18}$	pVL1352
pVL1819	*CEN URA3 yku80-8*$_{myc18}$	pVL1352
pRS306-*tlc1*-Δ*48*	*URA3 tlc1*-Δ*48*	48
pRS413	*CEN HIS3*	8
pSD120	*CEN URA3 TLC1*	D. Gottschling
pVL232	*CEN URA3 EST1*	47
pVL1312	*CEN LYS2 TLC1*	pVL317

Telomeric G-strand overhang assays. A *yku80*-Δ strain was transformed with *yku80^{tel}* mutant derivatives of pRS414 and wild-type and vector controls. After ~50 generations of growth, the transformants were grown to mid-log phase in selective media. Genomic DNA was isolated as previously described (22). DNA (25 to 40 μg) was either mock treated or treated with 40 U of *Escherichia coli* exonuclease I (Epicentre) in 100 μl of 50 mM Tris-HCl (pH 7.9), 10 mM $MgCl_2$, 100 mM NaCl, and 1 mM dithiothreitol for 15 min at 37°C. The reaction was stopped, and the DNA was precipitated with the addition of sodium acetate and ethanol. Following *Xho*I digestion, the DNA was resuspended in 12 μl of 10 mM Tris-HCl (pH 7.9), 10 mM $MgCl_2$, 50 mM NaCl, and 1 mM dithiothreitol. One microliter of 5′ ^{32}P-end-labeled dCCCACCACACACACCCACACCC (100,000 cpm/μl) was added, and hybridization was performed by a 10-min incubation at 37°C followed by 1 h on ice. The samples were applied to an agarose gel and electrophoresed at 22 V, and the gels were subsequently dried. Following detection of the single-strand telomeric signal, the gel was denatured and rehybridized with the same oligonucleotide probe, as previously described (12). The extent of alteration in each strain was quantified by normalizing, relative to a *YKU80* strain, the ratio of the native gel signal to the denatured gel signal for the Y′-containing telomeric restriction fragment (TRF). The native to denatured TRF signals were determined by densitometry and ImageQuant analysis for experiment 1 and PhosphorImager and ImageQuant analysis for experiment 2 (Table 3).

Protein level determination. A *yku80*-Δ strain was transformed with plasmids containing untagged *YKU80*, *YKU80*$_{myc18}$, and *yku80-1*$_{myc18}$ through *yku80-8*$_{myc18}$. Protein extracts were prepared (56), and Western blot analysis was performed as previously described (17). The protein levels were quantitated by densitometry and ImageQuant analysis. For a protein loading control, the membranes were reprobed with mouse anti-3′ phosphoglycerokinase (3′PGK) antibody (Molecular Probes). The level of Yku80 protein was normalized to the level of 3′PGK protein for each extract and then normalized to the wild type.

Chromatin immunoprecipitation assays. A *yku80*-Δ strain was transformed with plasmids containing untagged *YKU80*, *YKU80*$_{myc18}$, and *yku80-4*$_{myc18}$. Chromatin immunoprecipitation assays were performed on mid-log phase cultures as previously described (1), except that input and immunoprecipitated DNA were analyzed by Southern hybridization with a poly(dGT-dAC) probe to detect telomeric sequence and a TyB probe to detect background association. The signal was detected by PhosphorImager and quantitated with ImageQuant.

Alignment of the yeast and human proteins. An alignment between Yku80 and the human Ku80 protein structure was obtained by using GenTHREADER, version 4.5, a fold recognition method (25). The algorithm also incorporates secondary structure predictions determined by PSIPRED (26). The diagram of Ku bound to DNA (protein database identification, 1JEY) (61) was rendered by using Swiss PDB Viewer and POV-Ray.

RESULTS

Identification of *yku80^{tel}* mutations that are proficient for DNA repair but defective for telomere end protection. A model that reconciles the presence of Ku at telomeres, which are resistant to end-to-end fusion events, and DSBs, where Ku is required for end joining, is one in which Ku performs different functions at the different termini. In order to test this model, we screened for mutations in *YKU80* that separate roles for the Ku heterodimer in DNA repair from those in telomere function. Specifically, we screened for *yku80* mutants that conferred a severe growth defect when combined with a telomerase deficiency but were still proficient for DNA repair as assessed by an in vivo plasmid repair assay. A mutagenized *YKU80* plasmid library was introduced into a *yku80*-Δ *tlc1*-Δ/p*TLC1* yeast strain, and ~16,000 yeast transformants were screened for inviability after loss of the covering *TLC1* plasmid. Candidates that passed this test were subsequently screened for the ability to recircularize a linearized plasmid vector (see Materials and Methods and below for further details). This two-tiered screening strategy led to the identification of four mutations, called *yku80^{tel}* mutations, that retained the ability to repair DSBs but were defective for one or more functions required to maintain chromosome termini.

Figure 1 demonstrates that DNA repair was largely intact in these four mutant strains, as measured by two independent assessments of how cells handle DSBs. The first assay monitored in vivo repair of a plasmid linearized with the enzyme *Eco*RI (7, 40). Strains were transformed with a mixture of linearized and supercoiled plasmids with unique selectable markers, and recircularization of the linearized vector was measured as the number of transformants recovered with this vector relative to the supercoiled plasmid. This was performed in a *rad52*-Δ background in order to eliminate homologous recombination-mediated repair between the linearized plasmid and vector sequences on the plasmid carrying the *yku80^{tel}* mutation. The ability of a *yku80*-Δ strain to repair a linearized plasmid was down >25-fold compared to a *YKU80* strain (Fig. 1A), consistent with previous observations that loss of Ku function severely impairs the end joining of a linear DNA molecule (6, 40). In contrast, the *yku80^{tel}* mutants had either wild-type or close to wild-type levels of DNA repair (*yku80-3* and *yku80-4*)

TABLE 3. Summary of DNA repair and telomere properties of *yku80*^{tel} mutants

Allele[a]	Mutation	IVPRA[b]	HO assay result[c]	Growth in telomerase-null mutant[d]	G-tail detection[e] in:		Telomere length (bp)[f]	Telomeric silencing[g]
					Expt 1	Expt 2		
YKU80	None	1.0	+++	++	1.0	1.0	~320	Intact
yku80-1	L240S	0.53 ± 0.08	+++	−	7.9	11.4	~270	Abolished
yku80-4	P437L	1.33 ± 0.12	+++	−/+	8.0	5.9	~270	Impaired
yku80-2	Y49H	0.50 ± 0.10	+++	−/+	6.8	7.3	~265	Impaired
yku80-3	M16I	0.72 ± 0.15	+++	+/−	6.2	6.2	~280	Impaired
yku80-5[h]	Δaa 1–15	NQ	+++	+	4.6	6.8	~290	Impaired
yku80-6	S363P	NQ	+++	+	3.8	4.6	~290	Impaired
yku80-7	P437S	NQ	+++	+	6.0	6.2	~290	Impaired
yku80-8	L149R	NQ	+++	+(+)	2.0	1.7	~285	Impaired
yku80-Δ	None	<0.05 ± 0.01	−	−	15.4	24.2	~145	Abolished

[a] Alleles are ordered relative to the severity of their end protection defect, as assessed by growth in a telomerase-null strain and extent of G-tail defect.
[b] IVPRA, in vitro plasmid repair assay. For alleles *yku80-5* through *yku80-8*, the assay was performed but not to a sufficiently quantitative degree. NQ, nonquantitative.
[c] +++, wild type-appearing growth; −, no growth.
[d] Relative growth phenotypes, where ++ indicates healthy wild-type appearing colonies, +(+) indicates healthy appearing colonies with a small subpopulation of smaller colonies, +, +/−, and −/+ indicate increasing degrees of senescence with decreasing plating efficiency and increasing ragged colony and microcolony formation, and − indicates no growth.
[e] Native TRF signal/denatured TRF signal ratio normalized to that of the wild type. Results are reported for two independent experiments.
[f] $G_{1-3}T$ tract length.
[g] Altered refers to the ability to form colonies on both −Ura and 5-FOA media.
[h] Reduced protein levels.

or levels that were reduced by no more than twofold (*yku80-1* and *yku80-2*).

As a second measure of DNA repair proficiency, we determined the viability of the mutant strains when the HO endonuclease was constitutively expressed in a genetic background where both *HML* and *HMR* were deleted. In this genetic context, repair of an HO-induced DSB at the *MAT* locus is dependent upon the NHEJ pathway, such that survival is reduced 100- to 500-fold in the absence of Ku (30). As shown in Fig. 1B, these four *yku80*^{tel} strains behaved like a *YKU80* strain, whereas a *yku80*-Δ strain exhibited a severe defect (the additional four *yku80*^{tel} alleles shown in Fig. 1B will be discussed in a later section of this paper). Therefore, based on these two different measurements of DNA repair, each of the four *yku80*^{tel} mutant alleles retained the ability to rejoin a DSB.

Although DNA end-joining activity was largely retained, these mutant strains exhibited a set of phenotypes that indicate that they were impaired for the ability to protect chromosome termini. Previous work has shown that a strain that contains null mutations in both *YKU80* and telomerase can be propagated for only ~25 generations (43). This synthetic near-lethality has been proposed to result from the loss of the ability to both replicate and protect chromosome ends (43, 49; Bertuch and Lundblad, submitted). Thus, as a first step in determining whether the *yku80*^{tel} mutants had a chromosome end protection defect, we examined the growth characteristics of these four alleles when combined with a telomerase deficiency. Diploid strains containing integrated versions of each of the four *yku80*^{tel} mutations and an *est1*-Δ mutation were sporulated, and the viability of 4 to 5 haploid *yku80*^{tel} *est1*-Δ single colonies were assessed for each allele. As shown in Fig. 2A, *yku80*^{tel} *est1*-Δ strains exhibited a striking reduction in viability compared to an *est1*-Δ strain. Each of the *yku80*^{tel} *est1*-Δ strains behaved comparably to a *yku80*-Δ *est1*-Δ strain, in that they also could not be propagated beyond ~25 to 30 generations. Similar results were obtained when the double-mutant strains were generated by a plasmid shuffle: all four alleles again conferred greatly impaired growth when combined with either an *est1*-Δ mutation (Fig. 2B) or a *tlc1*-Δ mutation (data not shown). Because the plasmid shuffle protocol assesses growth at an earlier time point, this alternative assay also revealed that the *yku80-2 est1*-Δ, *yku80-3 est1*-Δ, and *yku80-4 est1*-Δ mutant strains were not quite as impaired as a *yku80*-Δ *est1*-Δ null mutant, although subsequent propagation of these double-mutant strains resulted in lethality (data not shown).

These results suggested that the ability to protect chromosome termini was impaired in these mutant strains. Consistent with this prediction, molecular analysis demonstrated that the structure of the ends of the chromosomes was altered in all four *yku80*^{tel} mutants. In wild-type yeast strains, the G-rich strand terminates as a single-strand extension that can be readily detected only in late S-phase (62). However, in *yku80*-Δ strains, end structure regulation is perturbed, such that single-stranded termini are present throughout the cell cycle (20, 49). Therefore, although G-tails can barely be detected in genomic DNA prepared from wild-type asynchronous cultures, such termini are readily detected in preparations from asynchronous *yku80*-Δ cultures (20, 49) (Fig. 2C). Similarly, all four of the *yku80*^{tel} mutants also exhibited readily detectable single-stranded G-rich DNA in asynchronous cultures (Fig. 2C). The signal was sensitive to the *E. coli* 3′-to-5′ exonuclease I, indicating that it corresponded entirely to the presence of G-rich single-stranded terminal overhangs. Quantitation of the extent of the increase in single-stranded signal (see Materials and Methods and Table 3) indicated a rough correlation with the growth defect in a telomerase-defective background: the *yku80-1*, which showed the most severe growth defect when combined with a telomerase mutation, also reproducibly

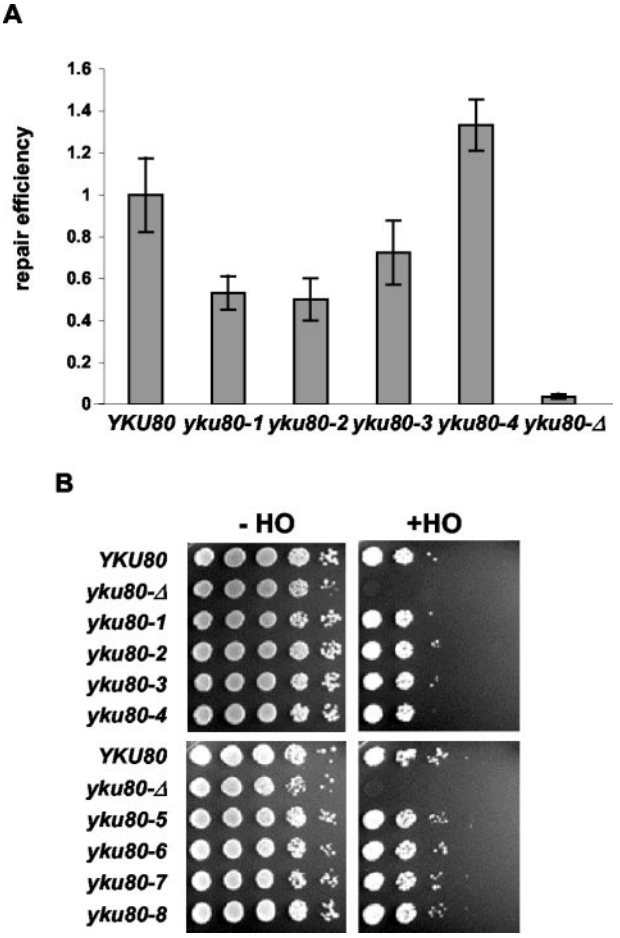

FIG. 1. *yku80*^{tel} mutants are proficient for repair of DSBs. (A) In vivo plasmid repair assay. A *yku80*-Δ *rad52*-Δ haploid strain bearing plasmid-borne *yku80*^{tel} mutant alleles was transformed with a mixture containing *Eco*RI, linearized pRS413 (*CEN HIS3*), and supercoiled pRS415 (*CEN LEU2*). Mutant alleles were tested in parallel with wild-type *YKU80* and vector controls. The repair efficiency is the Ura$^+$/Leu$^+$ transformant ratio normalized to that of *YKU80*. The results are the averages of the results of 2 to 4 transformations per strain from three separate experiments. Each error bar represents one standard deviation. (B) Continuous HO expression assay. Plasmids bearing *yku80*^{tel} mutant alleles were transformed into YVL2073 (*yku80*-Δ::*kan*^{r} *hml*-Δ::*ADE1 hmr*-Δ::*ADE1 ADE3*::*GAL*:*HO*) (Table 1). Tenfold serial dilutions were plated onto −Leu media containing either glucose (indicated −HO, which represses expression of the HO endonuclease) or galactose (indicated +HO, which induces expression of the HO endonuclease). Mutant alleles were tested in parallel with wild-type *YKU80* and vector controls.

displayed the largest increase in single-stranded signal. The *yku80-3* allele, which had the least severe growth defect, reproducibly displayed less of an increase in single-stranded signal. Therefore, these genetic and molecular criteria are consistent with the conclusion that chromosome end structure is altered in the four *yku80*^{tel} mutants. This argues that although DSBs are still repaired normally via Ku-dependent NHEJ, telomeres have become unprotected in these *yku80*^{tel} mutant strains.

One possible explanation for the separation of function displayed by these four alleles was that the level of Ku80 activity required for DNA repair was lower than the activity required for chromosome end protection. However, the steady state level of Yku80 protein in these four mutant strains was similar to that of the wild type, as monitored by Western analysis of epitope-tagged versions of each of mutant proteins relative to Yku80-myc18 (Fig. 2D). In addition, overexpression of the mutant Yku80-1 and Yku80-4 proteins did not rescue the synthetic lethality with telomerase (data not shown). Moreover, further analysis of the *yku80-4* mutant revealed that the Yku80-4 protein associated with telomeric chromatin at levels close to those of the wild type, as measured by a chromatin immunoprecipitation assay (Fig. 2E). Thus, the severe telomere phenotype exhibited by this allele was not due to the failure of the Yku80-4 mutant protein to associate with chromosome ends, nor could it be rescued by increased levels of mutant protein.

The role of *YKU80* in telomeric end protection is distinct from its role in telomere length regulation. Strains that completely lack either *YKU70* or *YKU80* function have short telomeric duplex tracts as well as altered G-tail regulation. To test whether these two changes in telomere structure could be the consequence of a single event, we examined telomere length in the four *yku80*^{tel} mutant strains, following propagation after ~65 generations to ensure that steady-state telomere lengths were reached in each strain. Telomeres were only slightly shortened in each of the four strains, in contrast to the severe telomere shortening observed in a *yku80*-Δ null strain (Fig. 3A and 2C and Table 3). This argues that despite the drastic change in end structure, Ku can still efficiently promote telomerase activity at chromosome termini in these four mutant strains.

As a reciprocal test, we examined a mutation in a subunit of yeast telomerase that is impaired for the Ku-mediated pathway of telomere length regulation. Ku regulates telomere length, in part, via an interaction with a stem-loop structure present in TLC1, the telomerase RNA subunit (48, 55). This Ku-specific regulatory activity is abolished in a *tlc1*-Δ*48* strain, which lacks this stem-loop, thereby resulting in short telomeres. However a *tlc1*-Δ*48* mutant strain was observed to have single-stranded G-rich extensions that were only slightly above that observed in a *TLC1* strain (Fig. 3B), showing that end structure was unaffected in a *tlc1*-Δ*48* strain. Thus, uncoupling the interaction of Ku with telomerase did not affect the ability of Ku to regulate telomere end structure. Therefore, the differential effects of the *tlc1*-Δ*48* mutant and the four *yku80*^{tel} mutants on telomere length versus G-tail extensions demonstrate that Ku regulates telomere length and terminal end structure by distinct activities.

The activity of the Ku heterodimer in chromosome end protection is distinct from its contribution to telomeric heterochromatin. In addition to mediating telomeric end protection and telomere length regulation, Ku also contributes to telomeric heterochromatin, as evidenced by the loss of repression of telomere-proximal genes (also referred to as telomeric position effect) in strains that lack Ku (5, 28, 43). To determine whether this constitutes a third, functionally distinct activity, we turned to a prior set of observations about the opposing roles of the Rif and Sir proteins in telomeric silencing. The Ku heterodimer has been proposed to influence heterochromatin formation by assisting the Sir proteins in their competition with the Rif proteins and the establishment of a repressive chromatin structure. Thus, in the absence of the Rif proteins, a role for

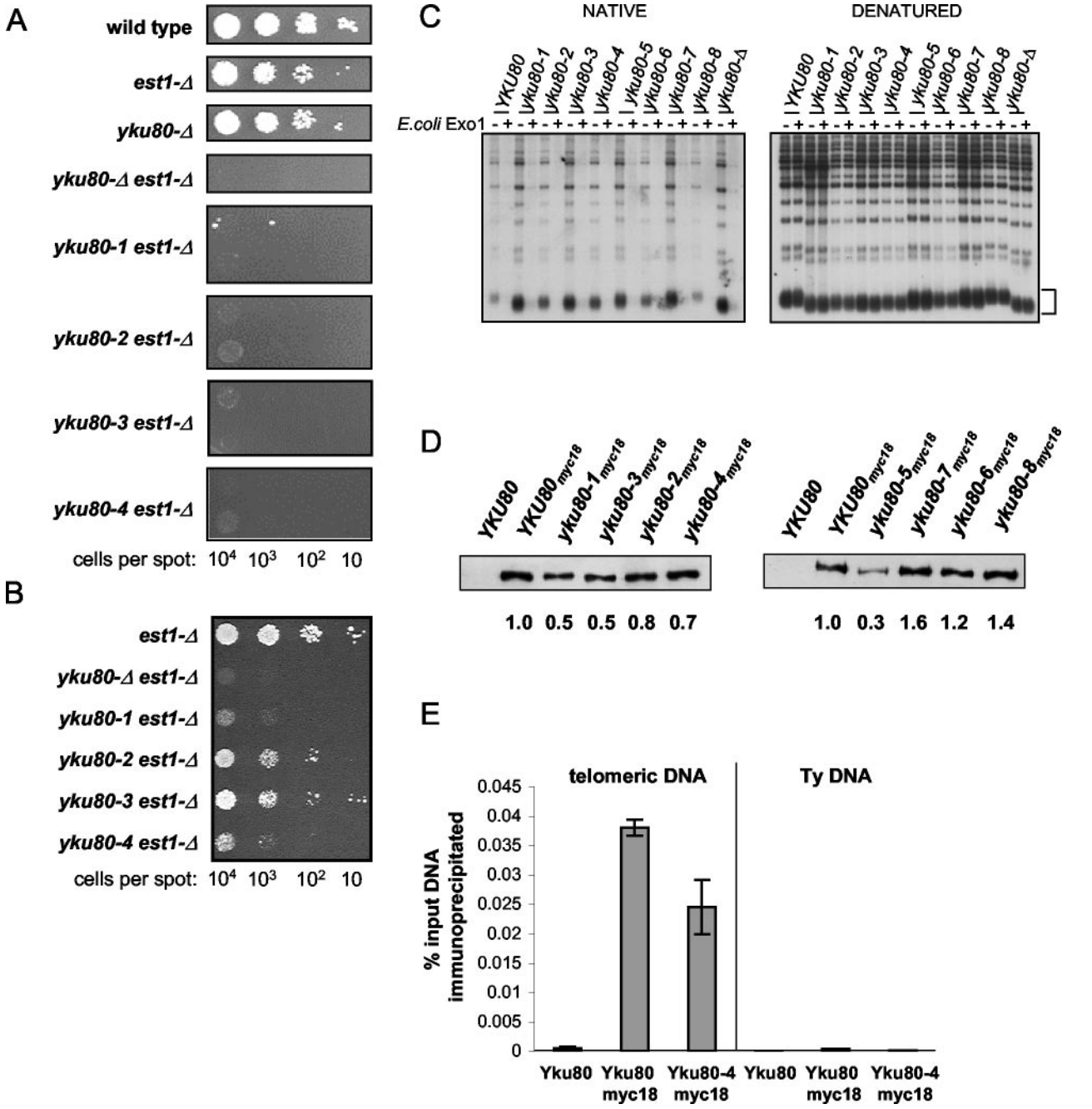

FIG. 2. *yku80*^{tel} mutants are defective for chromosome end protection. (A) Viability of *yku80*^{tel} *est1*-Δ double mutants generated by sporulation and dissection of the appropriate double heterozygous diploid (Table 1). Shown are 10-fold serial dilutions of equivalent numbers of cells taken directly from fresh dissection plates. (B) Viability of *yku80*^{tel} *est1*-Δ double mutants generated by plasmid shuffle. Plasmids (*CEN TRP1*) bearing *yku80*^{tel} mutant alleles were transformed into strain YVL1041 (*yku80*-Δ *est1*-Δ/p*CEN URA3 EST1*) (Table 1). Tenfold serial dilutions of equivalent numbers of cells were plated on −Trp 5-FOA media to evict the *EST1* covering plasmid. (C) Analysis of telomeric end structure. Plasmids bearing *yku80*^{tel} mutant alleles were introduced into a *yku80*-Δ strain. The DNA was mock treated (−) or treated with *E. coli* exonuclease 1 (+). (Left panel [native]) Detection of telomeric G-strand overhangs (see Materials and Methods). (Right panel [denatured]) Detection of total telomeric DNA. The same gel following in-gel denaturation and rehybridization with the same oligomeric probe. (D) Western blot analysis. Plasmids expressing either untagged *YKU80*, *YKU80*$_{myc18}$, or *yku80*$^{tel}_{myc18}$ alleles were transformed into a *yku80*-Δ strain. Equivalent amounts of protein from whole-cell extracts were analyzed by Western blotting with an anti-myc antibody or with an anti-3′PGK antibody. The levels of Yku protein were normalized to the levels of PGK protein (data not shown). (E) Chromatin immunoprecipitation. Plasmids expressing either untagged *YKU80*, *YKU80*$_{myc18}$, or *yku80-4*$_{myc18}$ alleles were transformed into a *yku80*-Δ strain. Following formaldehyde cross-linking, protein-DNA complexes were immunoprecipitated with anti-myc antibodies. Telomeric DNA and high-copy-number nonspecific control sequence DNA (TyB) were detected by Southern blotting. The average of the results from 3 to 4 assays is shown. Each error bar indicates one standard deviation.

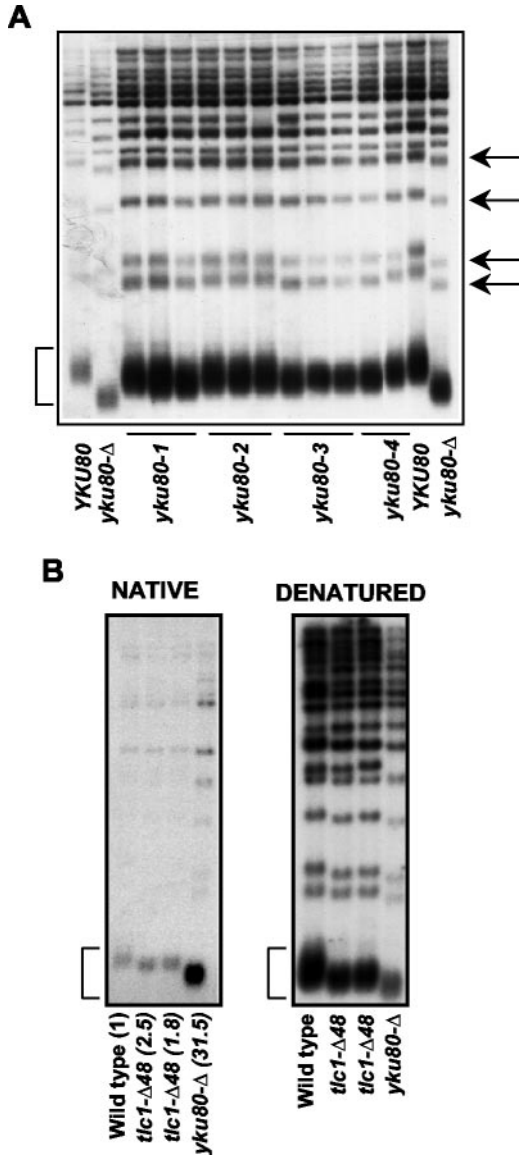

FIG. 3. Ku has separable functions in telomere length regulation and telomere end protection (A) Telomere length analysis of *yku80*^{tel} mutants. Plasmids bearing *yku80*^{tel} mutant alleles were transformed into a *yku80*-Δ strain. A Southern blot of genomic DNA isolated after ~65 generations of growth was probed to detect telomeric sequences. Independent isolates of each mutant allele were tested in parallel with wild-type *YKU80* and vector controls. The four bands marked by arrows represent individual telomeres. (B) Analysis of telomeric end structure in a *tlc1*-Δ*48* strain. Genomic DNA isolated from mid-log phase cultures of wild-type, *tlc1*-Δ*48*, and *yku80*-Δ strains. (Left panel [native]) Detection of telomeric G-strand overhangs. Indicated in parentheses is the native TRF signal/denatured TRF signal ratio normalized to that of the wild type. (Right panel [denatured]) Detection of total telomeric DNA.

Ku in telomeric silencing becomes dispensable, such that in a *yku70*-Δ *rif1*-Δ *rif2*-Δ strain, the telomeric silencing defect observed in a *yku70*-Δ strain is suppressed (41).

If the Ku heterodimer contributes a single function to telomere maintenance, loss of Rif protein function should similarly suppress the synthetic lethality observed in strains deficient in both Ku and telomerase. However, if Ku contributes separate activities to telomeric heterochromatin and telomeric end structure, loss of Rif proteins should not rescue the enhanced growth defect of a strain that lacks both Ku and telomerase. Consistent with this latter prediction, the *yku80*-Δ *rif1*-Δ *rif2*-Δ *est2*-Δ mutant strain exhibited a growth defect that was indistinguishable from that of the *yku80*-Δ *est*-Δ double mutant, since both sets of strains could only be propagated for ~25 generations (Fig. 4); the few *yku80*-Δ *rif1*-Δ *rif2*-Δ *est2*-Δ colonies that appeared had escaped lethality by utilizing a recombination-based mechanism of telomere maintenance (data not shown). As expected, *rif1*-Δ *rif2*-Δ *est2*-Δ mutant strains exhibited a senescence phenotype comparable to that of the *est2*-Δ strains, consistent with prior observations (57). Loss of *TLC1* function in a *yku80*-Δ *rif1*-Δ *rif2*-Δ strain showed results comparable to those shown in Fig. 4 (data not shown). Furthermore, the presence of terminal single-stranded G-tails in a *yku80*-Δ *rif1*-Δ *rif2*-Δ strain was comparable to that in a *yku80*-Δ strain, whereas little or no G-tail signal was detected in DNA prepared from *rif1*-Δ *rif2*-Δ mutant strains (reference 21 and data not shown). Thus, although loss of Rif protein function can suppress the telomeric silencing defect observed in *yku*-Δ mutant strains, the telomeric end protection defect is not Rif protein dependent. These results are consistent with the premise that Ku possesses a third telomere-specific activity.

Identification of four additional *yku80*^{tel} mutations by a second separation-of-function screening strategy. As an alternative approach to examine whether the Ku heterodimer contributes separable functions to telomeric end protection and telomeric silencing, we screened for an additional class of *yku80* alleles. Specifically, we asked whether we could identify mutations in *YKU80* that were defective for telomeric silencing but did not enhance the growth defect of a telomerase-deficient strain immediately following loss of a *TLC1* covering plasmid. In this second separation-of-function screen, a mutagenized *YKU80* plasmid library was introduced into a *yku80*-Δ strain that contained *ADE2* and *URA3* reporter genes placed next to a telomere, to permit telomeric silencing, and

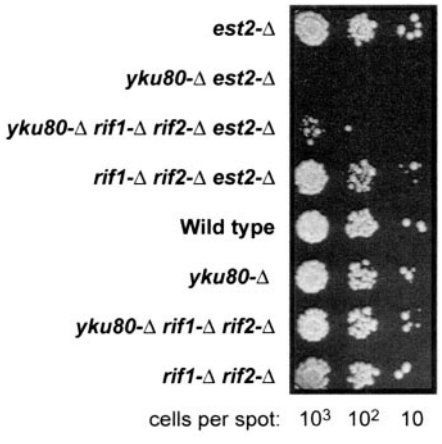

FIG. 4. Loss of Rif1 and Rif2 function does not rescue the growth defect of a *yku80*-Δ *est2*-Δ strain. Growth of isogenic haploid strains of the designated genotypes obtained by sporulation and dissection of YVL1071 (Table 1). Equivalent numbers of cells taken directly from the dissection plate were plated at a 10-fold serial dilution series.

thus the status of duplex telomeric chromatin, to be monitored. In addition, the strain contained a deletion of the genomic *TLC1* gene covered by a plasmid copy of *TLC1*, which allowed assessment of the growth phenotype after loss of the *TLC1* covering plasmid. Over 16,000 yeast transformants were screened for *yku80* alleles that resulted in expression of the normally repressed *ADE2* gene but did not enhance the senescence growth defect of a telomerase-defective strain following a plasmid shuffle (see Materials and Methods for details). This approach led to the identification of four additional *yku80^{tel}* mutations, *yku80-5* through *yku80-8*. Protein levels were not significantly altered in the *yku80-6*, *yku80-7*, and *yku80-8* strains (Fig. 2D), indicating that the silencing defect in these three strains appears to be due to a change in activity, rather than simply due to a reduction in protein levels. The levels of the Yku80-5 protein were reduced by about three- to fourfold, suggesting that at least some of the phenotypic consequences of this mutation may be due to reductions in the level of protein rather than a specific mutational alteration.

In contrast to the first set of *yku80^{tel}* mutations, initial analysis suggested that each of the four alleles from this second mutagenesis apparently failed to enhance the senescence phenotype of an *est1*-Δ mutant strain when examined for viability immediately following loss of a covering plasmid (Fig. 5A). This was expected, because lack of a phenotype in a telomerase-defective background immediately following loss of a covering *EST1* plasmid was part of the screening protocol used to recover these alleles. However, further propagation of *yku80-5 est1*-Δ, *yku80-6 est1*-Δ, *yku80-7 est1*-Δ, and *yku80-8 est1*-Δ strains revealed that these four *yku80* mutations conferred a noticeable synthetic growth defect in the presence of an *est1*-Δ null mutation when compared to a *YKU80 est1*-Δ strain (Fig. 5B, compare isolates grown for ~25 and ~50 generations). These effects were also observed when double-mutant *yku80^{tel} est1*-Δ strains were generated following dissection of a heterozygous diploid with integrated copies of the *yku80-6*, *yku80-7*, and *yku80-8* alleles (Fig. 5C).

The fact that there was an enhanced growth defect in the absence of telomerase suggested that telomeric end structure might also be at least partially impaired in this second set of mutants. In fact, the *yku80-5*, *yku80-6*, and *yku80-7* alleles showed an increase in the degree of single-strandedness at chromosomal termini that was roughly comparable to that observed in the *yku80-3* mutant strain (Fig. 2C and Table 3). The *yku80-8* strain had only a minimal impact on telomeric end structure: the degree of terminal single-strandedness in this strain was only slightly increased above that observed in a wild-type strain background, consistent with the fact that this mutant allele reproducibly exhibited a more modest effect in a telomerase-defective strain background (Fig. 5A to C and data not shown).

Notably, duplex telomere length exhibited only a minimal reduction in these four strains (30 to 35 bp) (Fig. 5D and Table 3). Therefore, like the first set of *yku80^{tel}* alleles, a marked alteration in end structure in *yku80-5*, *yku80-6*, and *yku80-8* strains was not accompanied by significant change in telomere length regulation.

As with the first set of four *yku80^{tel}* alleles, this second set of strains was also proficient for DNA repair. As shown in Fig. 1B, in vivo repair of DSBs induced by the HO endonuclease occurred at wild-type levels in *yku80-5* through *yku80-8.* Therefore, each of these four *yku80^{tel}* mutant alleles retained the ability to rejoin a DSB, just as was observed for the first set of *yku80^{tel}* mutants.

***yku80^{tel}* mutations alter telomeric position effect.** The second separation-of-function mutagenesis strategy was designed to uncover mutant alleles of *YKU80* that altered the effect of the Ku heterodimer on telomeric heterochromatin, as evidenced by its impact on telomeric position effect. Figures 5E and F illustrate that this second set of *yku80^{tel}* alleles exhibited marked effects on telomeric position effect. Three different assessments of telomeric silencing were performed. In the *YKU80* version of the strain background used, stable inheritance of transcriptionally repressed chromatin at the telomeric *URA3* locus prevents growth in the absence of uracil and allows growth on 5-FOA (2). Conversely, in a *yku80*-Δ strain, disruption of telomeric heterochromatin, and the consequent relief of repression of *URA3*, allows colony formation in the absence of uracil and prevents growth on 5-FOA (28, 43). Similarly, the chromatin status of a telomeric *ADE2* gene can be monitored: *YKU80* colonies, which have repressed *ADE2* expression, are red, whereas *yku80*-Δ colonies, which have a loss of telomeric silencing and have relief of *ADE2* repression, are white (28).

The four new *yku80^{tel}* mutant strains were equally able to form colonies in the absence of uracil with high efficiency (Fig. 5E, compare left and middle panels), indicating that the *URA3* gene was derepressed. An impairment in telomeric silencing in the *yku80^{tel}* strains was similarly observed when expression of an *ADE2* gene, located at a different telomere, was monitored. Similar to *yku80*-Δ colonies, *yku80-5* through *yku80-8* colonies were uniformly white (Fig. 5F), indicating that an open chromatin conformation was stably inherited in these mutant strains.

As an additional assessment of the impact of these *yku80^{tel}* alleles on telomeric heterochromatin, growth in the presence of 5-FOA was monitored. In contrast to the phenotype displayed by a *yku80*-Δ strain, the *yku80-5* through *yku80-8* mutant strains formed colonies when grown on media containing 5-FOA at a level comparable to that observed in a *YKU80* strain (Fig. 5E, compare left and right panels), indicating that the telomeric *URA3* gene could also be repressed in these mutant strains. Therefore, these three assays (growth in the absence of uracil, colony color, and growth in the presence of 5-FOA) indicate that telomeric silencing is greatly impaired in the *yku80-5* through *yku80-8* alleles, although not completely abolished.

Examination of the effects of the first set of *yku80^{tel}* alleles on telomeric silencing revealed that the *yku80-2*, *yku80-3*, and *yku80-4* strains showed a silencing defect very similar to that described above for *yku80-5* through *yku80-8*, whereas the *yku80-1* strain showed a silencing defect roughly comparable to that of the null mutant (Fig. 5E and data not shown). Thus, with the exception of *yku80-1* and *yku80-8*, six *yku80^{tel}* alleles all have a common set of phenotypes, despite the fact that they were recovered from two different screening strategies: these six mutant strains all disrupt telomeric end protection (although to various degrees) and have comparable effects on telomeric silencing.

The *yku80-8* strain appears to have a distinct set of properties: telomeric end protection is only marginally impaired, yet it exhibits the same telomeric silencing defect exhibited by the

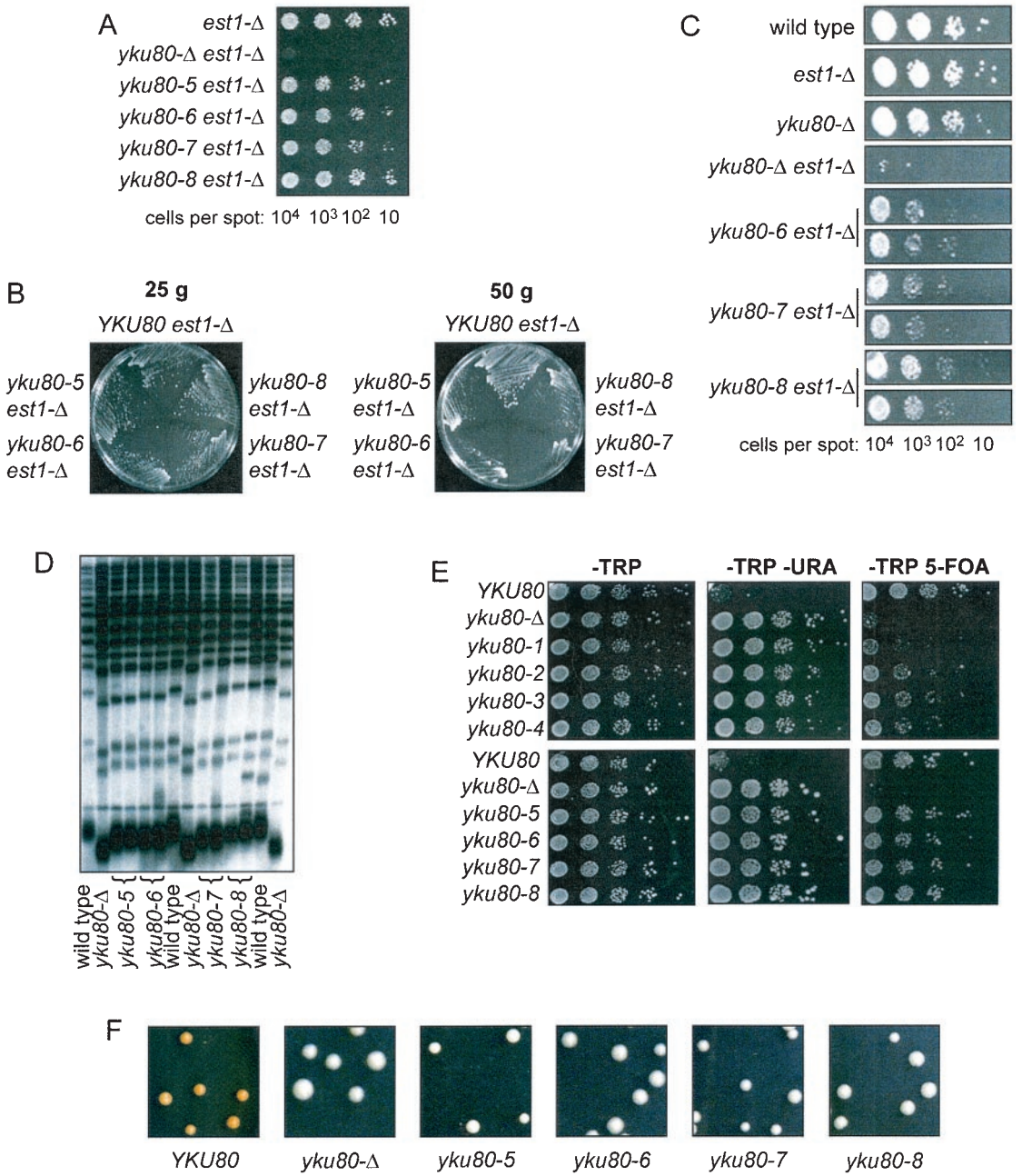

FIG. 5. *yku80-5* through *yku80-8* mutants are minimally impaired for telomere end protection but significantly impaired for telomeric silencing. (A) Viability of *yku80^{tel} est1*-Δ double mutants generated by plasmid shuffle. Plasmids (*CEN TRP1*) bearing *yku80^{tel}* mutant alleles, wild-type *YKU80*, and vector controls were introduced into strain YVL1041 (*yku80*-Δ *est1*-Δ/p*CEN URA3 EST1*) (Table 1). Tenfold serial dilutions of equivalent numbers of cells were plated onto −Trp 5-FOA media to evict the *EST1* covering plasmid. (B) Serial streakouts following loss of the *EST1* covering plasmid. The strains in panel A were streaked directly onto −Trp 5-FOA for single colonies (~25 generations of growth following loss of the *EST1* covering plasmid, left plate). Subsequently, single colonies were restreaked on −Trp (~50 generations, right plate). (C) Viability of *yku80^{tel} est1*-Δ double mutants generated by sporulation and dissection of the appropriate double heterozygous diploid (Table 1). Tenfold serial dilutions of equivalent numbers of cells obtained directly from the dissection plate were plated. (D) Telomere length analysis of *yku80^{tel}* mutants 5 through 8. Plasmids bearing *yku80^{tel}* mutant alleles, wild-type *YKU80*, and vector controls were transformed into a *yku80*-Δ strain. After ~65 generations, telomeric sequences were detected by Southern blot analysis of *Xho*I-digested genomic DNA. (E) Silencing of a telomere-located reporter *URA3* gene is altered in *yku80^{tel}* strains. Plasmids bearing *yku80^{tel}* mutant alleles were transformed into strain YVL885 (*yku80*-Δ *ppr1 ADE2*-TEL$_{VR}$ *URA3*-TEL$_{VIIL}$) (Table 1). Tenfold serial dilutions of cells were plated on −Trp media to determine plating efficiency (left), −Trp −Ura to evaluate the extent of *URA3* derepression (middle), and −Trp 5-FOA to evaluate the extent of *URA3* repression (right). Mutant alleles were tested in parallel with wild-type *YKU80* and vector controls. (F) A telomere-located reporter *ADE2* gene is stably derepressed in *yku80^{tel}* strains. Plasmids bearing *yku80^{tel}* mutant alleles and wild-type and vector controls were transformed into strain YVL885. Cells were plated on media selecting for the presence of the plasmid and limiting adenine to monitor *ADE2* expression by colony color.

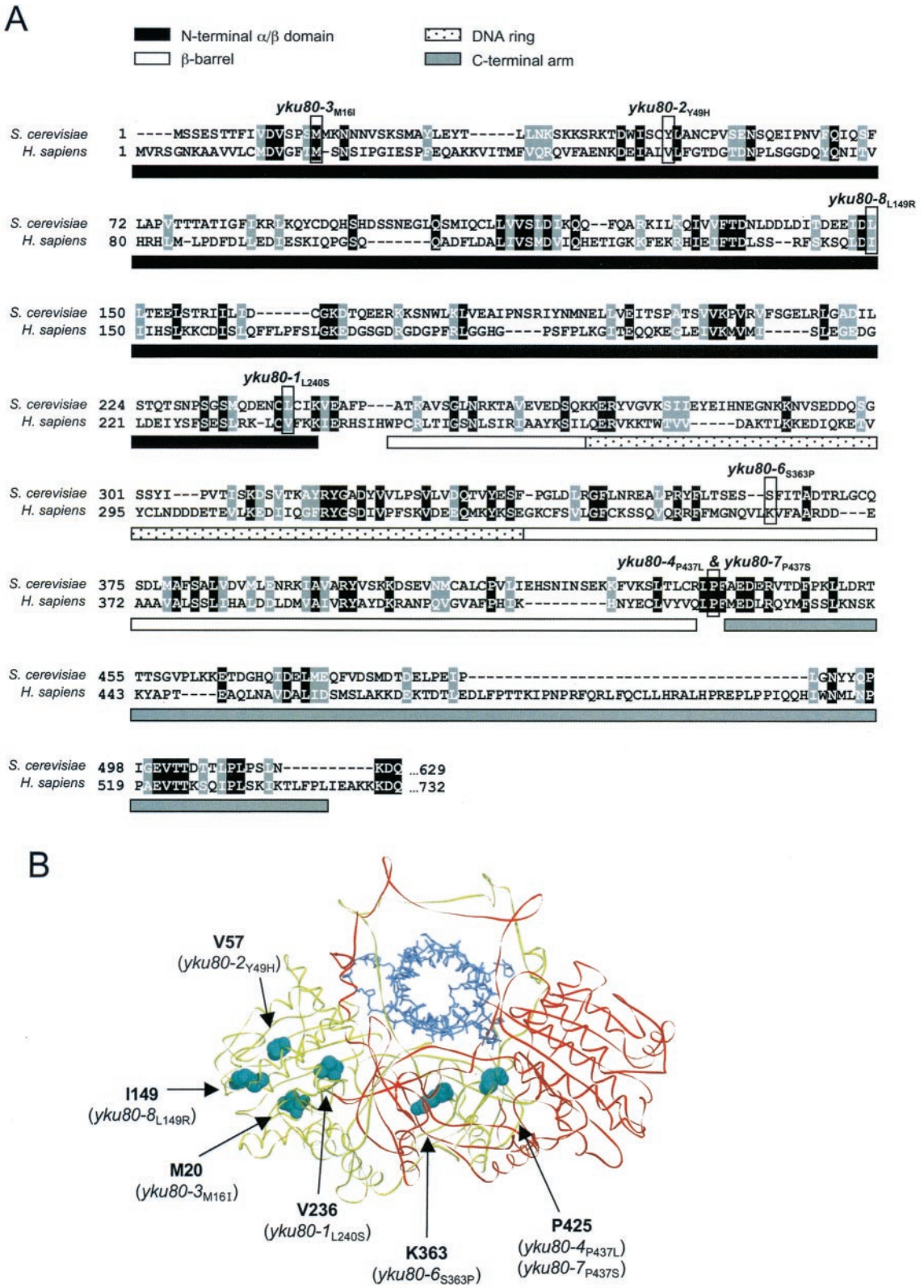

FIG. 6. A subset of the *yku80*^{tel} mutants map to residues that are conserved between *S. cerevisiae* and humans. (A) Alignment of the *S. cerevisiae* Ku80 and human Ku80 proteins with secondary structure and fold recognition programs (see Materials and Methods). Alignment to the last 188 aa of the human Ku80 protein was not included, as this portion was lacking in the structural determination (61). Identical residues are shaded in black, and similar residues are shaded in gray. Positions of the *yku80*^{tel} missense mutants are indicated. The domains of the human Ku80 structure (61) are delineated by bars below the sequence. (B) Position of human Ku80 residues that correspond to the *yku80*^{tel} mutations mapped on a diagram based on crystal structure of Ku bound to DNA (61). Ku80 and Ku70 are shown in yellow and red, respectively, and DNA is in blue. The predicted positions of the yeast *yku80*^{tel} alleles are shown as cyan-colored space-filled residues.

other *yku80^{tel}* strains. Thus, the properties of the *yku80-8* allele lends further support to the premise that telomeric silencing represents a third discrete activity performed by the Yku80 protein.

***yku80^{tel}* alleles target amino acid residues conserved between yeast and human Yku80 proteins.** DNA sequencing revealed that seven of the *yku80^{tel}* mutant alleles are the result of single amino acid substitutions (Fig. 6 and Table 3). The remaining allele (*yku80-5*) is due to a single nucleotide substitution in the initiating methionine codon, which predicts that the Yku80-5 mutant protein initiates protein synthesis at M16, with the consequent loss of 15 aa from the N terminus. Strikingly, the two different mutant screens recovered two alleles that altered the same amino acid. The *yku80-4* mutation was the consequence of a P → L missense mutation at residue 437, whereas the *yku80-7* mutation was due to a P → S alteration at the same position.

The Ku heterodimer functions in telomere maintenance in both yeast and mammalian cells. In order to determine whether the *yku80^{tel}* mutants implicated conserved residues between the two proteins, we sought to determine where the comparable amino acid residues mapped on the human Ku80 structure. Sequence identity among Ku80 proteins across diverse species is low, which precludes an unambiguous alignment between the human and yeast proteins. In order to address this, secondary structure prediction (PSIPRED) (26) and fold recognition (GenTHREADER) (25) methods were used to generate a structure-based alignment between the yeast and human Ku80 proteins (61). The amino acid alignment revealed that five *yku80^{tel}* alleles are due to mutations in four residues that are either identical or similar between the yeast and human proteins (*yku80-1*, *yku80-3*, *yku80-4*, *yku80-7*, and *yku80-8*) (Fig. 6A). Furthermore, the structure-based alignment permitted determination of mapping of the *yku80^{tel}* mutations to the various Ku80 domains. Five mutations (*yku80-1*, *yku80-2*, *yku80-3*, *yku80-5*, and *yku80-8*) mapped to residues on the human Ku structure within the N-terminal α/β domain (Fig. 6). The *yku80-6* mutation mapped to the β barrel domain, and the *yku80-4* and *yku80-7* mutations mapped to a conserved proline in the linker region between the β barrel and the C-terminal arm. Notably, none of the eight mutations map to residues that contact DNA.

DISCUSSION

Separable functions for Ku in DSB repair and telomere maintenance. Previous work has established a critical role for the Ku heterodimer in both DNA end joining and telomere maintenance. While there has been progress in elucidating the molecular mechanisms by which Ku carries out its role at DSBs, its activity at the telomere has remained elusive. This is due in part to the multiple telomere-related phenotypes present in Ku-deficient strains and the paucity of mutant alleles with which to probe telomere function. Toward understanding Ku's role at the telomere, we have conducted two mutant screens, which together yielded eight informative alleles of *YKU80*. Detailed analysis of NHEJ and telomere structure and function in these mutant strains, combined with epistasis arguments, lead us to two general conclusions: (i) Ku's role at ends created by DNA breaks is different from its role at telomeric ends and (ii) Ku has multiple separable functions at telomeres.

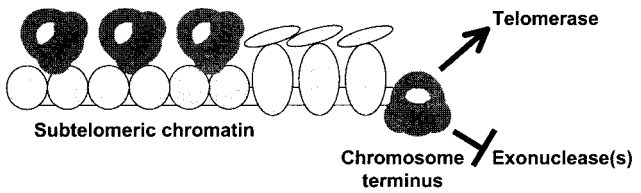

FIG. 7. A model for separable functions for Ku at the telomere. Ku associates with subtelomeric chromatin, where it influences the formation of heterochromatin. Independently, Ku associates with the chromosome terminus, where it mediates telomere length regulation via interactions with telomerase and telomere end protection via inhibition of an end-processing activity.

All eight of the alleles identified in this work were proficient at NHEJ but had defects in various aspects of telomere function, demonstrating that the type of end influences Ku's molecular function. These results also imply that at least one biochemical activity, the ability to bind DNA ends, was not altered, which is consistent with the fact that none of the *yku80^{tel}* mutations map to residues involved in DNA binding. In seven of the *yku80^{tel}* strains, telomere length regulation was minimally perturbed, whereas terminal DNA structure was significantly altered and senescence was accelerated in the absence of telomerase. In contrast, the *yku80-8* strain was significantly disrupted for telomeric position effect but maintained telomere length and telomere end structure at near wild-type levels. Therefore, these eight alleles support a model in which Ku mediates its activity in telomere length regulation, telomere end protection, and telomeric silencing via different mechanisms.

A simple model to explain the multiple roles for Ku in these aspects of telomere structure and function is presented in Fig. 7. We propose that the Ku heterodimer performs discrete sets of functions at chromosome termini and at duplex subtelomeric chromatin, and as a result, we suggest that Ku separately interacts with these two locations (possibly at temporally distinct periods during the cell cycle). This aspect of the model is supported by both the phenotypes of the *yku80-8* allele and the differential effects of *rif11*Δ *rif2*-Δ mutations on the silencing and end protection defects of Ku-deficient strains. Furthermore, while at the chromosome terminus, we propose that Ku participates in two different activities: it facilitates telomerase-mediated G-strand synthesis, thereby contributing to telomere length regulation, and it separately protects against resection of the C-strand, thereby contributing to protection of chromosome termini. Loss of the first activity results in telomere shortening, whereas loss of the second activity leads to alterations in chromosome end structure (i.e., constitutive G-tails). The phenotypes of the *yku80^{tel}* and *tlc1-Δ48* alleles support this aspect of the model, in that the *yku80^{tel}* mutants alter the terminal end structure but telomere length is maintained, whereas the *tlc1-Δ48* mutant has short telomeres but telomere end structure is unperturbed.

The idea that these multiple distinct activities correspond to different molecular interactions mediated by Ku at chromosome termini is supported by several prior observations. Ku has been shown to be responsible for protecting telomeric ends

from nuclease action: in the absence of YKu70, ExoI gains access to deprotected termini and results in degradation of the C-rich strand, which extends into subtelomeric regions (37). In contrast, Ku's role in telomere length regulation is mediated through an interaction with a stem-loop structure of the TLC1 RNA subunit of telomerase (48, 55) and may additionally require a function provided by the Est1 telomerase subunit (17).

Whereas Ku may execute its chromosome terminus-specific roles by interacting with terminal telomeric DNA, we propose that Ku associates with duplex subtelomeric chromatin via protein-protein associations (Fig. 7). It is at these subtelomeric sites that Ku performs activities that affect heterochromatin formation. Consistent with this model, Ku's influence on the recruitment of Sir4 appears to be restricted to subtelomeric sites, where it modulates the spreading of heterochromatin through this region (35, 41, 59).

Homology modeling suggests structure-function relationships of Yku80. Homology modeling with the crystal structure of the human Ku-DNA complex (61) reveals that *yku80-1*, *yku80-2*, *yku80-3*, and *yku80-8* mutations map to residues within the N-terminal α/β domain (Fig. 6B). In addition, *yku80-5* truncates the N-terminal 15 aa of this domain. The N-terminal α/β domain has been previously proposed to be a binding site for other repair factors (61). We propose that this region may also be critical for telomere-specific interactions.

Two alleles (*yku80-4* and *yku80-7*) alter a conserved proline residue in the linker between the β-barrel and C-terminal arm, a domain that contains extensive contacts with the Ku70 subunit (Fig. 6B). Thus, these mutations could potentially influence the positioning of the C-terminal arm and, as a consequence, alter interactions either between the Ku80 and Ku70 subunits or with additional telomere-specific proteins. Given that NHEJ is intact in the Yku80^{tel} mutant proteins, one might speculate that if these mutations weaken heterodimer stability, this would not be detrimental to Ku's role in NHEJ, where Ku association is transient (38). In contrast, stable association of the Ku heterodimer to telomeric DNA may be critical for its functions at the telomere. Therefore, the alterations imposed by the *yku80-4* and *yku80-7* mutations may impair the stability of the Ku heterodimer and, hence, its stable association with the telomere at all phases of the cell cycle. Biochemical analysis is in progress to determine whether the Yku80-4–Yku70 or Yku80-7–Yku70 protein complexes do in fact exhibit reduced stability.

Prior support for separable functions for the Ku heterodimer come from the identification of C-terminal truncation mutants of YKu70 protein subunit that are defective in certain aspects of telomere maintenance but proficient for NHEJ (13). However, for these mutants, simultaneous high-copy expression of the various Yku70 mutant proteins and the Yku80 protein could fully or nearly fully suppress the telomere defects of the *yku70* truncation alleles, suggesting a defect related to protein stability rather than molecular function. Therefore, this leaves open the question of whether the C-terminal 25-aa region of the Yku70 protein possesses a telomere-specific activity or simply modulates it.

Universal role(s) for Ku at telomeres. Review of the consequences of a Ku deficiency in different species provides an interesting comparison with the separation-of-function analysis reported here. For example, in *Schizosaccharomyces pombe*, in contrast to *S. cerevisiae*, Ku is not required for telomeric silencing (36). Nonetheless, Ku is required for telomere length regulation in both species (4, 36). In *Arabidopsis*, there is no evidence of telomeric fusions in the absence of Ku (52), in contrast to the marked increase in end-to-end fusions observed in Ku-deficient mouse cells (3, 9, 24, 53). Together, these observations indicate that subsets of Ku-specific functions have been separated evolutionarily in certain species.

Interestingly, Ku80-deficient mice are growth retarded and display both cellular and organismal early onset of senescence (45, 60). In addition, Ku80 is essential in human somatic cells, with apoptotic cell death occurring after a limited number of population doublings (33). The extent to which these phenotypes in mouse and human cells are secondary to defects in DSB repair versus loss of telomere end protection may be addressed with the generation of Ku separation-of-function mutants analogous to those described here for yeast cells.

ACKNOWLEDGMENTS

We thank Nathan Walcott, Monika Walterscheid, Priya Kayath, Pinaki Patel, Olive Botor, and Amy Aroopala for technical assistance; Kara Nyberg and Ted Weinert for sharing their G-tail protocol; and Jeff Bachant, Jim Haber, and Dan Gottschling for generously providing strains and plasmids. Special thanks go to Deborah Wuttke for comments on the Ku80 protein alignment and Srinivasan Madubushi for assistance with rendering the Ku structure. We also thank members of the Lundblad lab for helpful discussions and Rachel Cervantes, Jim Huang, and Deborah Wuttke for critical reading of the manuscript.

This work was supported by a Baylor College of Medicine Child Health Research Center New Project Development Award (to A.B.), NIH grant K08 HD01231 (to A.B.), and NIH grant R01 AG16626 (to V.L.).

REFERENCES

1. **Aparicio, O. M.** 1999. Characterization of protein bound to chromatin by immunoprecipitation from whole-cell extracts, p. 21.3.1–21.3.12. *In* F. M. Ausubel, R. Brent, R. E. Kingston, D. D. Moore, J. G. Seidman, J. A. Smith, and K. Struhl (ed.), Current protocols in molecular biology. John Wiley & Sons, Inc., New York, N.Y.
2. **Aparicio, O. M., and D. E. Gottschling.** 1994. Overcoming telomeric silencing: a trans-activator competes to establish gene expression in a cell cycle-dependent way. Genes Dev. **8:**1133–1146.
3. **Bailey, S. M., J. Meyne, D. J. Chen, A. Kurimasa, G. C. Li, B. E. Lehnert, and E. H. Goodwin.** 1999. DNA double-strand break repair proteins are required to cap the ends of mammalian chromosomes. Proc. Natl. Acad. Sci. USA **96:**14899–14904.
4. **Baumann, P., and T. R. Cech.** 2000. Protection of telomeres by the Ku protein in fission yeast. Mol. Biol. Cell **11:**3265–3275.
5. **Boulton, S. J., and S. P. Jackson.** 1998. Components of the Ku-dependent non-homologous end-joining pathway are involved in telomeric length maintenance and telomeric silencing. EMBO J. **17:**1819–1828.
6. **Boulton, S. J., and S. P. Jackson.** 1996. Identification of a *Saccharomyces cerevisiae* Ku80 homologue: roles in DNA double strand break rejoining and in telomeric maintenance. Nucleic Acids Res. **24:**4639–4648.
7. **Boulton, S. J., and S. P. Jackson.** 1996. *Saccharomyces cerevisiae* Ku70 potentiates illegitimate DNA double-strand break repair and serves as a barrier to error-prone DNA repair pathways. EMBO J. **15:**5093–5103.
8. **Christianson, T. W., R. S. Sikorski, M. Dante, J. H. Shero, and P. Hieter.** 1992. Multifunctional yeast high-copy-number shuttle vectors. Gene **110:** 119–122.
9. **d'Adda di Fagagna, F., M. P. Hande, W. M. Tong, D. Roth, P. M. Lansdorp, Z. Q. Wang, and S. P. Jackson.** 2001. Effects of DNA nonhomologous end-joining factors on telomere length and chromosomal stability in mammalian cells. Curr. Biol. **11:**1192–1196.
10. **de Lange, T.** 2002. Protection of mammalian telomeres. Oncogene **21:**532–540.
11. **de Vries, E., W. van Driel, W. G. Bergsma, A. C. Arnberg, and P. C. van der Vliet.** 1989. HeLa nuclear protein recognizing DNA termini and translocating on DNA forming a regular DNA-multimeric protein complex. J. Mol. Biol. **208:**65–78.
12. **Dionne, I., and R. J. Wellinger.** 1996. Cell cycle-regulated generation of single-stranded G-rich DNA in the absence of telomerase. Proc. Natl. Acad. Sci. USA **93:**13902–13907.

13. **Driller, L., R. J. Wellinger, M. Larrivee, E. Kremmer, S. Jaklin, and H. M. Feldmann.** 2000. A short C-terminal domain of Yku70p is essential for telomere maintenance. J. Biol. Chem. **275:**24921–24927.
14. **DuBois, M. L., Z. W. Haimberger, M. W. McIntosh, and D. E. Gottschling.** 2002. A quantitative assay for telomere protection in *Saccharomyces cerevisiae.* Genetics **161:**995–1013.
15. **Dynan, W. S., and S. Yoo.** 1998. Interaction of Ku protein and DNA-dependent protein kinase subunits with nucleic acids. Nucleic Acids Res. **26:**1551–1559.
16. **Espejel, S., S. Franco, S. Rodriguez-Perales, S. D. Bouffler, J. C. Cigudosa, and M. A. Blasco.** 2002. Mammalian Ku86 mediates chromosomal fusions and apoptosis caused by critically short telomeres. EMBO J. **21:**2207–2219.
17. **Evans, S. K., and V. Lundblad.** 2002. The Est1 subunit of Saccharomyces cerevisiae telomerase makes multiple contributions to telomere length maintenance. Genetics **162:**1101–1115.
18. **Feldmann, E., V. Schmiemann, W. Goedecke, S. Reichenberger, and P. Pfeiffer.** 2000. DNA double-strand break repair in cell-free extracts from Ku80-deficient cells: implications for Ku serving as an alignment factor in non-homologous DNA end joining. Nucleic Acids Res. **28:**2585–2596.
19. **Ferguson, D. O., and F. W. Alt.** 2001. DNA double strand break repair and chromosomal translocation: lessons from animal models. Oncogene **20:** 5572–5579.
20. **Gravel, S., M. Larrivee, P. Labrecque, and R. J. Wellinger.** 1998. Yeast Ku as a regulator of chromosomal DNA end structure. Science **280:**741–745.
21. **Gravel, S., and R. J. Wellinger.** 2002. Maintenance of double-stranded telomeric repeats as the critical determinant for cell viability in yeast cells lacking Ku. Mol. Cell. Biol. **22:**2182–2193.
22. **Hoffman, C. S., and F. Winston.** 1987. A ten-minute DNA preparation from yeast efficiently releases autonomous plasmids for transformation of *Escherichia coli.* Gene **57:**267–272.
23. **Hsu, H. L., D. Gilley, E. H. Blackburn, and D. J. Chen.** 1999. Ku is associated with the telomere in mammals. Proc. Natl. Acad. Sci. USA **96:**12454–12458.
24. **Hsu, H. L., D. Gilley, S. A. Galande, M. P. Hande, B. Allen, S. H. Kim, G. C. Li, J. Campisi, T. Kohwi-Shigematsu, and D. J. Chen.** 2000. Ku acts in a unique way at the mammalian telomere to prevent end joining. Genes Dev. **14:**2807–2812.
25. **Jones, D. T.** 1999. GenTHREADER: an efficient and reliable protein fold recognition method for genomic sequences. J. Mol. Biol. **287:**797–815.
26. **Jones, D. T.** 1999. Protein secondary structure prediction based on position-specific scoring matrices. J. Mol. Biol. **292:**195–202.
27. **Kabotyanski, E. B., L. Gomelsky, J. O. Han, T. D. Stamato, and D. B. Roth.** 1998. Double-strand break repair in Ku86- and XRCC4-deficient cells. Nucleic Acids Res. **26:**5333–5342.
28. **Laroche, T., S. G. Martin, M. Gotta, H. C. Gorham, F. E. Pryde, E. J. Louis, and S. M. Gasser.** 1998. Mutation of yeast Ku genes disrupts the subnuclear organization of telomeres. Curr. Biol. **8:**653–656.
29. **Lee, S. E., J. K. Moore, A. Holmes, K. Umezu, R. D. Kolodner, and J. E. Haber.** 1998. Saccharomyces Ku70, Mre11/Rad50 and RPA proteins regulate adaptation to G2/M arrest after DNA damage. Cell **94:**399–409.
30. **Lee, S. E., F. Paques, J. Sylvan, and J. E. Haber.** 1999. Role of yeast *SIR* genes and mating type in directing DNA double-strand breaks to homologous and non-homologous repair paths. Curr. Biol. **9:**767–770.
31. **Lendvay, T. S., D. K. Morris, J. Sah, B. Balasubramanian, and V. Lundblad.** 1996. Senescence mutants of *Saccharomyces cerevisiae* with a defect in telomere replication identify three additional *EST* genes. Genetics **144:**1399–1412.
32. **Lewis, L. K., and M. A. Resnick.** 2000. Tying up loose ends: nonhomologous end-joining in *Saccharomyces cerevisiae.* Mutat. Res. **451:**71–89.
33. **Li, G., C. Nelsen, and E. A. Hendrickson.** 2002. Ku86 is essential in human somatic cells. Proc. Natl. Acad. Sci. USA **99:**832–837.
34. **Lundblad, V., and J. W. Szostak.** 1989. A mutant with a defect in telomere elongation leads to senescence in yeast. Cell **57:**633–643.
35. **Luo, K., M. A. Vega-Palas, and M. Grunstein.** 2002. Rap1-Sir4 binding independent of other Sir, yKu, or histone interactions initiates the assembly of telomeric heterochromatin in yeast. Genes Dev. **16:**1528–1539.
36. **Manolis, K. G., E. R. Nimmo, E. Hartsuiker, A. M. Carr, P. A. Jeggo, and R. C. Allshire.** 2001. Novel functional requirements for non-homologous DNA end joining in *Schizosaccharomyces pombe.* EMBO J. **20:**210–221.
37. **Maringele, L., and D. Lydall.** 2002. ExoI-dependent single-stranded DNA at telomeres activates subsets of DNA damage and spindle checkpoint pathways in budding yeast *yku70*Δ mutants. Genes Dev. **16:**1919–1933.
38. **Martin, S. G., T. Laroche, N. Suka, M. Grunstein, and S. M. Gasser.** 1999. Relocalization of telomeric Ku and SIR proteins in response to DNA strand breaks in yeast. Cell **97:**621–633.
39. **McEachern, M. J., A. Krauskopf, and E. H. Blackburn.** 2000. Telomeres and their control. Annu. Rev. Genet. **34:**331–358.
40. **Milne, G. T., S. Jin, K. B. Shannon, and D. T. Weaver.** 1996. Mutations in two Ku homologs define a DNA end-joining repair pathway in *Saccharomyces cerevisiae.* Mol. Cell. Biol. **16:**4189–4198.
41. **Mishra, K., and D. Shore.** 1999. Yeast Ku protein plays a direct role in telomeric silencing and counteracts inhibition by rif proteins. Curr. Biol. **9:**1123–1126.
42. **Nick McElhinny, S. A., C. M. Snowden, J. McCarville, and D. A. Ramsden.** 2000. Ku recruits the XRCC4-ligase IV complex to DNA ends. Mol. Cell. Biol. **20:**2996–3003.
43. **Nugent, C. I., G. Bosco, L. O. Ross, S. K. Evans, A. P. Salinger, J. K. Moore, J. E. Haber, and V. Lundblad.** 1998. Telomere maintenance is dependent on activities required for end repair of double-strand breaks. Curr. Biol. **8:**657–660.
44. **Nugent, C. I., T. R. Hughes, N. F. Lue, and V. Lundblad.** 1996. Cdc13p: a single-strand telomeric DNA-binding protein with a dual role in yeast telomere maintenance. Science **274:**249–252.
45. **Nussenzweig, A., C. Chen, V. da Costa Soares, M. Sanchez, K. Sokol, M. C. Nussenzweig, and G. C. Li.** 1996. Requirement for Ku80 in growth and immunoglobulin V(D)J recombination. Nature **382:**551–555.
46. **Pang, D., S. Yoo, W. S. Dynan, M. Jung, and A. Dritschilo.** 1997. Ku proteins join DNA fragments as shown by atomic force microscopy. Cancer Res. **57:**1412–1415.
47. **Pennock, E., K. Buckley, and V. Lundblad.** 2001. Cdc13 delivers separate complexes to the telomere for end protection and replication. Cell **104:**387–396.
48. **Peterson, S. E., A. E. Stellwagen, S. J. Diede, M. S. Singer, Z. W. Haimberger, C. O. Johnson, M. Tzoneva, and D. E. Gottschling.** 2001. The function of a stem-loop in telomerase RNA is linked to the DNA repair protein Ku. Nat. Genet. **27:**64–67.
49. **Polotnianka, R. M., J. Li, and A. J. Lustig.** 1998. The yeast Ku heterodimer is essential for protection of the telomere against nucleolytic and recombinational activities. Curr. Biol. **8:**831–834.
50. **Porter, S. E., P. W. Greenwell, K. B. Ritchie, and T. D. Petes.** 1996. The DNA-binding protein Hdf1p (a putative Ku homologue) is required for maintaining normal telomere length in *Saccharomyces cerevisiae*. Nucleic Acids Res. **24:**582–585.
51. **Ramsden, D. A., and M. Gellert.** 1998. Ku protein stimulates DNA end joining by mammalian DNA ligases: a direct role for Ku in repair of DNA double-strand breaks. EMBO J. **17:**609–614.
52. **Riha, K., J. M. Watson, J. Parkey, and D. E. Shippen.** 2002. Telomere length deregulation and enhanced sensitivity to genotoxic stress in Arabidopsis mutants deficient in Ku70. EMBO J. **21:**2819–2826.
53. **Samper, E., F. A. Goytisolo, P. Slijepcevic, P. P. van Buul, and M. A. Blasco.** 2000. Mammalian Ku86 protein prevents telomeric fusions independently of the length of TTAGGG repeats and the G-strand overhang. EMBO Rep. **1:**244–252.
54. **Singer, M. S., and D. E. Gottschling.** 1994. *TLC1*: template RNA component of *Saccharomyces cerevisiae* telomerase. Science **266:**404–409.
55. **Stellwagen, A. E., Z. W. Haimberger, J. R. Veatch, and D. E. Gottschling.** 2003. Ku interacts with telomerase RNA to promote telomere addition at native and broken chromosome ends. Genes Dev. **17:**2384–2395.
56. **Strahl-Bolsinger, S., A. Hecht, K. Luo, and M. Grunstein.** 1997. *SIR2* and *SIR4* interactions differ in core and extended telomeric heterochromatin in yeast. Genes Dev. **11:**83–93.
57. **Teng, S. C., J. Chang, B. McCowan, and V. A. Zakian.** 2000. Telomerase-independent lengthening of yeast telomeres occurs by an abrupt Rad50p-dependent, Rif-inhibited recombinational process. Mol. Cell **6:**947–952.
58. **Treco, D., and V. Lundblad.** 1993. Basic techniques of yeast genetics, p. 13.1.1–13.1.7. *In* F. M. Ausubel, R. Brent, R. E. Kingston, D. D. Moore, J. G. Seidman, J. A. Smith, and K. Struhl (ed.), Current protocols in molecular biology, vol. 2. John Wiley & Sons, Inc., New York, N.Y.
59. **Tsukamoto, Y., J. Kato, and H. Ikeda.** 1997. Silencing factors participate in DNA repair and recombination in *Saccharomyces cerevisiae.* Nature **388:** 900–903.
60. **Vogel, H., D. S. Lim, G. Karsenty, M. Finegold, and P. Hasty.** 1999. Deletion of Ku86 causes early onset of senescence in mice. Proc. Natl. Acad. Sci. USA **96:**10770–10775.
61. **Walker, J. R., R. A. Corpina, and J. Goldberg.** 2001. Structure of the Ku heterodimer bound to DNA and its implications for double-strand break repair. Nature **412:**607–614.
62. **Wellinger, R. J., A. J. Wolf, and V. A. Zakian.** 1993. Saccharomyces telomeres acquire single-strand TG1–3 tails late in S phase. Cell **72:**51–60.